Ocean Sci. Discuss., 6, 2005–2036, 2009
www.ocean-sci-discuss.net/6/2005/2009/

Ocean Science Discussions

Papers published in *Ocean Science Discussions* are under open-access review for the journal *Ocean Science*

Statistical trend analysis and extreme distribution of significant wave height from 1958 to 1999 – an application to the Italian Seas

G. Martucci[1], S. Carniel[2], J. Chiggiato[2], M. Sclavo[2], P. Lionello[3], and M. B. Galati[3]

[1]School of Physics & Centre for Climate and Air Pollution Studies, Environmental Change Institute, National University of Ireland, Galway, UK
[2]CNR-ISMAR, Castello 1364/A, 30122 Venice, Italy
[3]University of Lecce, Dep. of Material Sciences, Via Arnesano, 73100 Lecce, Italy

Received: 27 August 2009 – Accepted: 28 August 2009 – Published: 8 September 2009

Correspondence to: G. Martucci (giovanni.martucci@nuigalway.ie)

Published by Copernicus Publications on behalf of the European Geosciences Union.

Abstract

The study is a statistical analysis of sea states timeseries derived using the wave model WAM forced by the ERA-40 dataset in selected areas near the Italian coasts. For the period 1 January 1958 to 31 December 1999 the analysis yields: (i) the existence of a negative trend in the annual- and winter-averaged sea state heights; (ii) the existence of a turning-point in late 70's in the annual-averaged trend of sea state heights at a site in the Northern Adriatic Sea; (iii) the overall absence of a significant trend in the annual-averaged mean durations of sea states over thresholds; (iv) the assessment of the extreme values on a time-scale of thousand years. The analysis uses two methods to obtain samples of extremes from the independent sea states: the *r-largest annual maxima* and the *peak-over-threshold.* The two methods show statistical differences in retrieving the return values and more generally in describing the significant wave field. The study shows the existence of decadal negative trends in the significant wave heights and by this it conveys useful information on the wave climatology of the Italian seas during the second half of the 20th century.

1 Introduction

This study aims at performing a climatological and statistical analysis of the wave fields around the Italian coasts. In oceanography as well as in meteorology, climate can be described by the mean type, frequency and intensity of weather events occurring during a climatological period of time. The same way the mean values of a timeseries are used to assess the existence of a trend over a climatological time interval, the sample of the timeseries extremes is used to determine the probability of extreme events to occur at fixed return periods. Motivations to set the extreme events as a matter of study by environmental sciences have become increasingly impellent also due to the numerous applications of these studies, ranging from flood discharges, hurricane winds or storm surge to heavy precipitations, extreme temperatures and long period of summer

OSD

6, 2005–2036, 2009

or winter droughts. The aim of preventing extreme events to harm people and infrastructures determined a decided interest of the scientific community in understanding extreme events and reducing the uncertainty related to their assessment. The statistical analysis of the extreme waves is used by coastal engineers to assess the risk of damages to offshore constructions or by oceanographers and modellers to calculate trends in the past and future wave fields (Lionello et al., 2007), also based on different emission scenarios (Nakienovi et al., 2000).

Depending on the method and criteria to sample the extremes from a timeseries, different results can be obtained by applying the same statistical analysis on the different samples. Depending on the method and on the average value of the extremes, a specific event can be regarded as to be an actual risk for the environment or not. This suggests adopting a common policy across the scientific community aimed at defining methods, criteria and meanings of *extreme analysis*. The need to define a physical threshold to indicate whether an extreme could be or not a risk for the environment didn't bring to establish standard criteria of definition yet. Generally, it is hardly possible to set a unique threshold to select extremes from a very large dataset, e.g. a wind speed of 15 m/s could be a reasonable threshold for a region in which the peak speeds never exceed 25 m/s, but not for a region exposed to wind gusts of 40 m/s. A way to break this apparent deadlock is to work on methods instead of thresholds. The hitherto extreme wave analysis allows extracting the independent and identically-distributed (*iid*) data from climatological timeseries and to use them for applications of two methods such as the "peak over threshold" (POT, Hosking and Wallis, 1987; Smith, 1989; Davison and Smith, 1990; Abild et al., 1992; Simiu and Heckert, 1996) and the *r*-largest annual maxima (*r*max, Weissman, 1978; Smith, 1987) which are amongst the best techniques to select the extreme from large datasets and to provide robust estimates of the extreme values at future return periods.

In the next sections the analysis will focus on trends of the mean wave significant heights and durations over threshold and their related statistical significance on selected locations around the Italian coasts during the second half of the 20th century.

The statistical differences in the extreme analysis observed using the two methods will be used to assess which technique can provide the best return values for the selected return periods. The calculation of trends of significant wave height and the assessment of the probability of extreme waves to occur at fixed return periods, allow understanding the impact of the wave field on coastal areas.

2 Data setup and calibration

WAM is an advanced third generation model (WAMDI-Group, 1988) developed in the late 80s and presently one of the most widely used and tested by the scientific community (Komen et al., 1994). It calculates directional spectra from which integrated values such as significant wave height, mean wave direction and frequency can be derived.

Since July 1992 the European Centre for Medium-Range Weather Forecasts (ECMWF) runs WAM forced by a meteorological model. The re-analysis project ERA-40 (Uppala et al., 2005), completed in 2003, is an elaboration of the results of the hybrid T159 (~125 km) meteorological model covering the period from mid-1957 to mid-2002. A run of WAM forced by the ERA-40 wind fields was performed by the Department of Science of Materials, University of Lecce (Italy) for the period 1957–1999, covering the whole Mediterranean basin at 0.5° resolution. The wave dataset (further named "ERA-40$_{\mathrm{UNILE}}$") was obtained extracting the relevant information at selected points of the WAM output grid close to the Italian coasts (Fig. 1).

As highlighted by previous studies (Cavaleri and Bertotti, 2004; Signell et al., 2005), a possible underestimate of the wind speed components due to a lack of resolving small, sharp scale features in the wind pattern, may affects the WAM-computed values of H_s. Cavaleri and Sclavo (2006) presented a study in which the WAM output wave fields (0.5° grid resolution) from 1 July 1992 to 30 June 2002 have been calibrated for several points in the Mediterranean Sea, following two successive validation-calibration steps. First, the ERS1-2 and the Topex/Poseidon satellites wave data have been validated using the wave dataset provided by the Italian Buoy Network (De Boni et al.,

OSD
6, 2005–2036, 2009

1993), then the WAM model data have been calibrated by comparison with satellite data, and finally tested for correlation with other observational data. In the present work, a similar procedure has been applied, ensuring for the period from 1992 to 2002, a good-quality wave height timeseries around the Italian coasts that in the following will be named as "ISMAR".

The ERA-40$_{\mathrm{UNILE}}$ has been calibrated as well on 27 representative geographical sites around the Italian coasts, selected among the available WAM output grid points (see Fig. 1). The grid points have been selected to investigate the three seas skirting the Italian coasts, the Adriatic (eastern coast), the Ionian (southern coast) and the Tyrrhenian (western coast). Special focus has been on the Northern Adriatic area, a region of great interest for the Venetian frail coastal system. The wave timeseries has length 42 yr going from 1 January 1958 to 31 December 1999. The overlapping period between the ERA-40$_{\mathrm{UNILE}}$ and ISMAR calibrated timeseries is 7.5 yr, from 1992 to 1999. For the calibration process only, the 3 h temporal resolution of the ERA-40$_{\mathrm{UNILE}}$ timeseries has been sub-sampled to 6 h in order to synchronize the ERA-40$_{\mathrm{UNILE}}$ and the ISMAR timeseries.

A preliminary test of feasibility was done using the power-law $H_{\mathrm{s}}^{\mathrm{ISMAR}}=a\cdot(H_{\mathrm{s}}^{\mathrm{ERA\text{-}40_{UNILE}}})^{b}$ instead of a linear regression, leading to values of b very close to unity. Then, at each selected position the two timeseries have been linearly fitted to retrieve the calibration factor a and the intercept c using the linear model $H_{\mathrm{s}}^{\mathrm{ISMAR}}=a\cdot H_{\mathrm{s}}^{\mathrm{ERA\text{-}40_{UNILE}}}+c$. Table 1 shows the values of parameters a and c for the 27 points along the coasts. Rather large differences in the values are due to the different positions of grid points around Italian coasts; when points on the WAM output grid are close to the shoreline, the underestimation is large due to shallow waters.

Once calibrated, the two timeseries are in good agreement during the overlapping time interval (almost 18% of the whole period). In Fig. 2 are shown the results of the comparison at two representative sites located along the Italian coast. The calibrated ERA-40$_{\mathrm{UNILE}}$ timeseries has then been processed retaining only independent wave events (Corsini et al., 2000). The *iid* events from the 3-h data have been selected on

OSD

6, 2005–2036, 2009

the basis of their autocorrelation coefficient, ρ, retaining data with $\rho \leq 0.1$ to preserve only the peak of each independent storm.

3 Methodology of statistical analysis

The identification of the best probability distribution $F(h)$ fitting to the sampled *iid*-data allows the determination of the extreme waves return values $H_s^{(n)}$, and return periods T_n, where n is the number of years. Two methods are used for sampling the extremes from *iid* data: the r-largest annual maxima ($r$max) and the "peak over threshold" (POT) method. The first is a selection of the largest r-maxima (r=5) during each year throughout the timeseries. The second method, widely used, makes use of a threshold to select records from a dataset. The POT method increases the available information by using more than the r-largest peaks per year. However, in practical applications the results are quite sensitive to the criteria adopted for peak selection.

Since the early 60's, when data from measurement of ocean waves became available, scientists started studying significant wave heights as a crucial variable using model distributions together with data observations (Draper, 1963). The best practice suggests selecting the significant wave height threshold based on the values of three parameters, i.e. season, geographical area and wave provenance. This procedure ensures that the threshold value depends directly on the wave timeseries. Once the data are sorted by period of the year, site and incoming direction each timeseries can be processed by selecting a threshold as a fixed percentile of the ordered wave height dataset.

Earlier studies (Isaacson and MacKenzie, 1981; Muir and El-Shaarawi, 1986; Mathiesen et al., 1994; Goda, 1997; Brabson and Palutikof, 2000) focused on the comparison of these two techniques, rarely providing an answer about which method is preferable. Actually, after POT and $r$max methods apply to the same *iid* sample, the resulting selected datasets are hardly fitted by the same probability distribution, $F(H_s)$. Each $F(H_s)$ distribution is fitted to the POT and $r$max datasets and, based on the least

squares method, only the distribution showing the highest correlation coefficient is selected. The choice of $F(H_s)$ is crucial to all determined outputs (e.g., durations over threshold and extreme values) since they depend on the shape of F.

A statistical analysis of the ERA-40$_{UNILE}$ wave timeseries has been performed (Sect. 3.1) to provide information about the annual winter averaged significant wave height (H_s), the significance of trends during the 42-yr period and the total number of wave events. The annual number of sea states, the annual- and the winter-averaged H_s and the statistical significance of their trends in the Northern Adriatic Sea are presented in Sect. 3.2. The annual-averaged mean H_s durations above three different thresholds and the statistical significance of their trends are studied in Sect. 3.3.The POT and the *r*max determined extreme waves are discussed in Sect. 3.4.

3.1 Trend in mean H_s value

The determination of a trend in the ERA-40$_{UNILE}$ timeseries is relevant when assessing the H_s future scenarios. Four grid points have been chosen to represent the three Seas on the North, South, East and West of Italy. For the northern area, the point (45.0° N, 13.0° E) has been selected instead of the one closer to Venice (45.5° N, 13.0° E) because of a significantly higher value of the correlation coefficient in the linear calibration procedure (linear wave timeseries correction). A linear fitting (Fig. 3a) shows the trend of the mean H_s value along the period of the ERA-40$_{UNILE}$ timeseries, obtained as an average over the winter period (December to February), i.e. when most of the sea storms occur. All sea states (all heights and directions) have been considered for the analysis that shows a clear negative trend in all the computed linear fits. Especially in the Adriatic Sea, trend's slopes through the 42 yr are negative being 4.5×10^{-3} m yr^{-1} and 4.2×10^{-3} m yr^{-1} for Northern and Middle Adriatic, respectively. A Student's *t* test has been used to assess the statistical significance of all trends. The null hypothesis of zero-slope is rejected for all the four cases at a 5%- level of significance. Trends in Fig. 3a are in agreement with the overall negative trends in winter averaged H_s values found by Lionello and Sanna (2005) over the Mediterranean Sea. Figure 3b shows the

OSD
6, 2005–2036, 2009

trends in the annual-averaged H_s values. Also in this case, the statistical significance of negative trends have been proved at the 5%-level. This piece of information will be useful to interpret results in Sect. 3.3.

Pirazzoli and Tomasin (2003) found, for the period 1951–1996, a general negative trend of the wind frequency and intensity at many stations along the Italian coasts. The authors particularly focused on the Adriatic Sea area finding a *turning-point* matching the end of a general negative trend (from 1951 up to mid 70's) and the beginning of a positive one lasting till the end of the dataset, in 1996. Since the wave and wind climate are strictly correlated, a deeper analysis has been performed of the Northern Adriatic data to understand more about the existence of such trends. Results are summarized in the next section.

3.2 Statistics and trend of Bora events in the Northern Adriatic Sea

The wave occurrences and heights have been statistically analyzed at several representative sites in the Northern Adriatic. This area, embedding the Venice lagoon and its coastal surroundings, is of particular interest due to the delicate equilibrium of its ecosystem that calls for a better understanding and mitigation of the wave impact. For the point in front of the Venetian coast (45.0° N, 13.0° E), Fig. 4 shows the height, occurrences and incoming direction of H_s divided in four decades (1960–69, 1970–79, 1980–89 and 1990–99). Data have been sampled using a threshold set at 0.5 m. Throughout the first three decades a general decrease in wave occurrences does happen in correspondence of both the incoming directions of *Bora* (north-easterly, down-sloping wind) and *Sirocco* (Mediterranean south-easterly wind). On the contrary, a moderate increase appears for the *Bora* data from 1990 to 1999; during the same period, the *Sirocco* component continues to decrease.

Actually, the number of times a wave comes from a certain direction and its significant height value are not, a priori, correlated; nonetheless, from further investigations on the data, a positive correlation can be inferred, as explained in Fig. 5. The total number of H_s counts and annual-averaged values for sea states H_s>0.5 m coming from the

OSD

6, 2005–2036, 2009

Bora sector (0° through East to 90°) are shown. The timeseries in both panels of Fig. 5 can split into two sub-series with turning-point around 1989. Two assumptions have been formulated about data shown in the upper and lower panel of Fig. 5. The first assumption says that the slopes of the two trends are both different from zero, the second that the means of the two trend population are different. To validate the assumptions two Student's t tests have been applied to both sub-series. The first test is based on the null-hypothesis that the two sub-series belong both to the zero-slope population, against the alternative hypothesis that the two slopes are different from zero. The second test is based on the null-hypothesis that the two sub-series belong both to the same μ-population (μ, mean value) against the alternative hypothesis that the mean values, μ_{32} (mean over 32 yr) and μ_{10} (mean over 10 yr), are different. Both Student's t have been computed at a 5%-level of significance with results summarised in Table 2. All the null-hypothesis have been rejected at this level of significance and then all trends in Fig. 5 are statistically reliable.

Looking at how data distribute in Fig. 5a, readers might identify other relatively long sub-trends of the wave occurrences, like the one in 1965–69 or the other in 1977–84. This is not the case for the annual averaged H_s shown in Fig. 5b, where the behaviour is roughly constant throughout the years except during 1989. If confirmed, the turning-point in 1977 (dashed circle in Fig. 5a) would be in good agreement with the trend turning-point observed for the wind in the mid 70s by Pirazzoli and Tomasin (at Venice Airport – 45°50′ N–12°33′ E, about 70 km from the studied point).

To evaluate the inferred turning-points, we compute a moving linear fit of 10-yr length of the data in Fig. 5a and b throughout the 42 yr. Results are shown in Fig. 6a and b where the ith data point (with i going from 1962 to 1994) represents the slope of the linear regression calculated over the period (i–4, i+5); error bars in both panels are equal to $\pm\sigma$ (one standard deviation). Analyzing Fig. 6a it comes out that a reverse positive trend (positive slope values) starts in 1978 and lasts up to 1983. Also from 1991 to 1994, slopes have a positive value, nevertheless, it is not possible to separate the two periods since the slope values are fully comparable within the interval $\pm\sigma$.

OSD
6, 2005–2036, 2009

Then, the positive trend outlined in Fig. 5a can not be regarded as (statistically) unique. On the contrary, in Fig. 6b from 1989 to 1994, slopes have values well above the confidence intervals of the previous years confirming that the positive trend shown for the last decade in Fig. 5b is (statistically) unique.

3.3 Trends of duration of the sea states over threshold

An evaluation of potentially dangerous storms for coastal activities should not consider the significant wave height as the only parameter responsible for damages to structures. Also the storm duration is a relevant issue for port engineering and offshore work installations (i.e., underwater cables or pipelines, oil-plants). Two approaches to calculate the storm duration over fixed thresholds are presented here. The first, the *triangular technique*, determines directly from the timeseries the cumulated and mean temporal interval $\tau(h)$ during which a sea state H_s lays above a certain threshold h. This technique linearly reconstructs a continuous sea state signal by interpolating the 6-h data. The second approach is based on a *parametric model* (Mathiesen, 1994) relying on the shape of the sea state samples (as selected by the POT or by the $r$max methods), the selected probability distribution $F(H_s)$ and the absolute mean temporal gradient of the original H_s timeseries.

Regardless of site and fetch, applying the *parametric model* to the data of this study it has been found that the $\tau(h)$ values were systematically underestimated if compared to the ones determined by the *triangular technique*. Moreover, though the *parametric model* can provide satisfactory results when the height classes are homogeneously distributed, the obtained values of $\tau(h)$ are strongly influenced by the choice of the normalizing factor and the suitability of the selected distributions. Due to this, the triangular technique has been preferred to the parametric model and has been applied to the data analyzed in the following.

In Fig. 7, the annual averaged H_s mean durations over three thresholds (the 50th, the 75th and the 90th percentiles of the ordered ERA-40$_{\text{UNILE}}$ timeseries) are shown for the same locations presented in Fig. 3a. For the four cases, the three selected

OSD
6, 2005–2036, 2009

thresholds correspond roughly to the values (0.5μ, μ, 2μ), where μ is the overall mean value of each H_s timeseries. Data in Fig. 7 have been linearly fitted and the resulting trend tested for statistical significance. The probability distribution used to test the trends was a two-tailed Student's t distribution with $N-2=40$ degrees of freedom with level of significance α fixed at 5%. Results (see Table 3) show that in only one case ("Middle Adriatic Sea", 50th percentile) the null-hypothesis of zero-slope was rejected. Besides, the storm duration over threshold can be used to show the probability of exceedance P_h calculated as the ratio of the cumulated number of hours a storm exceeds the threshold h to the total number of hours per year. This is shown in Fig. 8, for the same locations presented before in Fig. 3a. As for the annual averaged mean durations over threshold, also for the probability of exceedance P_h, the calculated slopes of the linear fits are mainly negative, especially in correspondence of the 50th percentile threshold (statistically significant). The annual probability to exceed the higher thresholds is always between 0 and 10%, with an average constant trend throughout the studied period. Quantitatively, though all the calculated slopes of the 50th percentile trend are negative and almost all those of the 90th percentile are positive (except for the "Northern Adriatic" case), a clear trend in the annual averaged H_s duration over threshold can not be inferred, except for one case. Qualitatively, even if most of the trends shown in Figs. 7 and 8 failed the significance test, it is possible to relate the results in these two figures to those obtained in Fig. 3a and b. For direct comparison to data in Figs. 7–8 only results from Fig. 3b will be discussed since they all originate from annual averages. Apart from the 90th percentile, all the calculated 50th and 75th percentile linear fit slopes are negative; this finds agreement with the negative trends in Fig. 3b. In fact, an analysis of the data used to produce results in Fig. 3b, reveals that the most relevant contribution to the averaging process comes from sea states with heights less than 1 m. This threshold corresponds approximately to the 75th percentile of the datasets. We can then expect that a long term negative trend in the mean H_s value, as the one observed in Fig. 3b, would affect directly the mean sea state durations above the 50th percentile threshold.

OSD

6, 2005–2036, 2009

It is finally possible to draw two conclusions on the analyzed trends, one based on the quantitative analysis and one based on a qualitative interpretation of the data in Figs. 3b and 7–8. The first conclusion is that, despite a clear decrease in the annual- and winter-averaged H_s values, during the last 40 yr, both the annual averaged duration over three different thresholds and the probability of exceeding these thresholds have shown no statistically significant trends. The second conclusion is that the durations and probabilities corresponding to the 50th and 75th percentiles are in agreement with the results shown in Fig. 3b i.e. the probability of exceeding a threshold h diminishes as the mean height of the sea states becomes smaller.

3.4 Extreme events

The comparison between POT and $r$max methods aims at defining which method can provide, for fixed return periods, the best estimation of the return values with the least statistical error. The set of cumulative probability distributions generally employed for the extreme data analysis are the Weibull (2 or 3 parameters), Fréchét, Gumbel or the Lognormal distributions. Since a Lognormal distribution can be represented by a Weibull distribution with one parameter set to a fixed value, a linear least squares based algorithm has been implemented, which selects automatically the best fitting distribution amongst the:

$$
\begin{aligned}
F(H_s) &= 1 - \exp\left[-\left(\frac{H_s - B}{A}\right)^{\gamma}\right] \qquad (\text{Weibull},\ B \le H_s < \infty),\\
F(H_s) &= \exp\left[-\left(1 + \frac{H_s - B}{\gamma A}\right)^{-\gamma}\right] \qquad (\text{Fréchét},\ B - \gamma A \le H_s < \infty), \qquad (1)\\
F(H_s) &= \exp\left[-\exp\left(-\frac{H_s - B}{A}\right)\right] \qquad (\text{Gumbel},\ -\infty \le H_s < \infty).
\end{aligned}
$$

Where, A, B and γ are, respectively, the *scale*, the *location* and the *shape* parameter. The A and B coefficients are determined using the linear least square methods,

OSD
6, 2005–2036, 2009

whereas the shape parameter γ assumes the values γ=0.75, 1.0, 1.4 and 2.0 (Goda, 1997). The best fitting distribution, as well as the shape parameter value, are then selected and used to compute the return values and periods of the extreme sea states, as well as their duration over threshold (Eq. 1). A threshold fixed at the 50th percentile of the ordered dataset and a value r=5 are used for the application of the POT and the $r$max methods, respectively. Different choices of the POT threshold or the annual maxima could have been performed leading to slightly different results. We decided to fix the threshold at the 50th percentile because this represents a neutral choice. A higher threshold, shifted towards the highest values of the dataset, would have been closer to the criteria of selection of $r$max, but would have carried a larger uncertainty to the obtained predictions.

A comparison between the two methods is shown in Fig. 9 for three different geographical sites representing each a coastal Italian area (Adriatic, Ionian and Tyrrhenian). The two methods provide closer estimations for return periods T_n>100 yr. For small return periods, the return values are larger using the $r$max method. Actually, data selected by the POT method are waves with height larger than the 50th percentile threshold and then POT sample contains waves with *non-extreme* heights too. Conversely, the $r$max method, selecting only extremes from the initial *iid* dataset, is a good candidate to provide more realistic extreme return values.

An assessment of the mean duration over thresholds, τ_n, of extreme waves with return value $H_s^{(n)}$ and return period T_n is given by the expression (Mathiesen, 1994):

$$\tau_n \left(H_s^{(n)}(T_n) \right) = \left(1 - F \left(H_s^{(n)}(T_n) \right) \right) \cdot T_n, \quad (2)$$

where, $H_s^{(n)}(T_n)$ is the height of a sea state with return period T_n and F is the non-exceedance probability of the ordered return values $H_s^{(n)}$. In Table 4 are given the values of τ_{100}=τ_n (T_n=100) and $H_s^{(100)}$ for both methods and for the three cases shown in Fig. 9. For the three presented cases, only in the middle panel the probability distribution is not the same for both methods, i.e. the $r$max sample is fitted by a Gumbel dis-

tribution. The 3-parameters Weibull distribution is always selected by the least square method when fitting to the POT sample. Black triangles in the graphics compare the highest maximum of the *iid* data with the return value determined by the extreme analysis in correspondence to the return period T=40 yr. If the maximum is an outlier, as for the case in panel (a), the return value for T=40 will hardly represent this maximum. This is because predictions by POT and *r*max methods are based on the values of the statistical probability distribution $F(h)$. This distribution fits to data sample and can not represent properly the outliers. Nevertheless, over the studied period, the related error to the failing prediction of one outlier occurs with a probability of ∼1/122 640. In all the considered cases, *r*max predicted the dataset highest wave better than POT.

Qualitatively, for T_n<100 yr, the *r*max method provides more realistic return values, despite a larger statistical error. When considering larger return periods (T_n>100 yr), the POT method gives return values comparable with the ones computed by *r*max, but with a smaller statistical error. This is explained by the fact that the differences between the two methods are larger for small return periods when extreme return values strongly depend on the source dataset. For large return periods, the POT dependence on source dataset becomes feeble and the method provides better extreme return values with a smaller standard deviation. Other studies about extreme events analysis support the notion that *r*max can provide trusty estimations of the return values (Tanurdjaja, 2002; Cook et al., 2003; Brink et al., 2004).

4 Conclusions

The first part of this study was dedicated to determine trends and statistical significances during the period from 1 January 1958 to 31 December 1999 for the ERA-40_{UNILE} wave timeseries, a calibration of WAM model outputs produced using the ERA-40 forcings. The investigated wave parameters were the H_s values (averaged over the winter season and over all the incoming directions); the total number of sea states characterised by a certain H_s for all the incoming directions (and particularly

OSD
6, 2005–2036, 2009

for the North-Eastern sector); the averaged mean duration and probability of threshold exceedance; the return periods of extreme waves and their duration of exceedance.

The statistical analysis showed that, during the second half of the 20th century winter averaged H_s had a statistically significant negative trend. These results are in agreement with those of Lionello and Sanna (2005).

An investigation of the existing relation between the observed decrease in the total number of occurrences and in the annual averaged values of H_s, was carried out through the period from 1960 to 1999, in the Northern Adriatic area. The results showed a clear negative trend during the first three decades opposite to a reverse positive trend starting with a turning-point at the beginning of the last decade. All the trends turned out to be statistically significant at the test level, nevertheless a less pronounced turning-point in 1977 suggested testing again the positive trend of the last decade. This procedure assured that only the trend in the annual averaged H_s values could be regarded as to be unique. These results well correlate with those obtained by Pirazzoli and Tomasin (2003).

A theoretical parametric model (Mathiesen, 1994) to determine the H_s mean duration over threshold was assessed by comparing the parametric values with those obtained applying the *triangular technique* to the ERA-40$_{UNILE}$ timeseries. The parametric model was found to generally underestimate the mean durations over thresholds (results of comparison not shown). The triangular technique has then been used to study the annual averaged values of the mean durations, $\tau(h)$, and the corresponding probabilities of exceedance (P_h) of the h-thresholds at the 50th, the 75th and the 90th-percentiles. Although the slopes in Figs. 7 and 8 did not satisfy the test of significance at the 5%-level, a qualitative interpretation of the data was made. The annual-averaged mean durations and the probabilities to exceed the 50th percentile-threshold have negative linear fit slopes, which fairly agrees with the negative trends obtained for the annual-averaged H_s in Fig. 3b, i.e. the probability of exceeding a threshold h diminishes as the mean height of the sea states is decreasing. If the overall negative trends will be confirmed in future years, being the wave energy related to H_s^2, the studied areas around

OSD

6, 2005–2036, 2009

the Italian coasts will be characterized by progressively less “energetic” conditions.

In the last part of the paper we compared two methods to select the extreme samples from the *iid* data, the POT and the *r*max. The presented cases showed differences in the computed extreme return values especially for return periods T_n<100 yr. In this range, the return values determined by POT were systematically smaller than the ones determined by the *r*max. For T_n>100 yr, the POT method can provide extreme return values closer to those computed by *r*max and with a smaller statistical error. In general, the *r*max method was preferable to the POT, especially for T_n<100 yr.

The obtained results also suggest a careful employment of the parametric model when calculating the mean duration of a sea state over threshold, and provide useful advice about which method between the POT and *r*max better represents the return values and periods.

Acknowledgements. This activity was supported by the research contract between ISMAR-CNR and Consorzio Venezia Ricerche, in the frame of CMCC Project, and by the VECTOR-FISR Project. Support from CNR-RSTL “MOM” is also acknowledged.

References

Abild, J., Andersen E. Y., and Rosbjerg D.: The climate of extreme winds at the Great Belt of Denmark, J. Wind Eng. Ind. Aerodyn., 41–44, 521–532, 1992.

Brabson, B. B. and Palutikof, J. P.: Tests of the Generalized Pareto Distribution for predicting extreme wind speeds, J. Appl. Meteorol., 39, 1627–1640, 2000.

van den Brink, H. W., Können G. P., and Opsteegh, J. D.: Statistics of extreme synoptic-scale wind speeds in ensemble simulations of current and future climate, J. Climate, 17, 4564–4574, 2004.

Cavaleri, L. and Bertotti, L.: Accuracy of modeled wind and wave fields in enclosed seas, Tellus, 56(2), 167–175, 2004.

Cavaleri, L. and Sclavo, M.: The Calibration of Wind Model Data in the Mediterranean Sea, Coast. Eng., 53, 613–627, 2006.

Coles, S.: An Introduction to Statistical Modeling of Extreme Values, Springer-Verlag, London, UK, 204 pp., 2001.

Cook, N. J., Harris, R. I., and Whiting, R.: Extreme wind speeds in mixed climates revisited, J. Wind Eng. Ind. Aerodyn., 91, 403–422, 2003.
Corsini, S., Guiducci, F., and Inghilesi, R.: Statistical Extreme Waves Analysis of the Italian Sea Wave Network measurement data in the period 1989–1999. 10th International Offshore And Polar Engineering Conference, 3, 137–143, 2000.
Davison, A. C. and Smith, R. L.: Models of exceedances over high thresholds, J. Roy. Stat. Soc. B Met., 52, 339–442, 1990.
De Boni, M., Cavaleri, L., and Rusconi, A.: The Italian wave measurement network, 23rd Int. Conf. Coast. Eng., Venice, 4–9 October 1992, 116–128, 1993.
Draper, L.: Derivation of a design wave, Instrum. Rec. Sea Waves Proc. Inst. Civ. Eng., 26, 291–304, 1963.
Goda, Y.: Statistical Analysis of Extreme Waves. Part III of Random Seas and Design of Maritime Structures, 443 pp., Advanced Series on Ocean Engineering – 15, World Scientific, 1997.
Harris , R. I.: Gumbel revisited – a new look at extreme value statistics applied to wind speeds, J. Wind Eng. Ind. Aerodyn., 59, 1–22, 1996.
Hosking, J. R. and Wallis, J. R.: Parameter and quantile estimation for the generalized Pareto distribution, Technometrics, 29, 339–349, 1987.
de Isaacson, M. St. Q. and MacKenzie, N. G.: Long-Term Distribution of Ocean Waves: A Review, J. Waterway Port Coast, Ocean Div., 107(WW2), 93–109, 1981.
Komen, G. J., Cavaleri, L., Donelan, M., Hasselmann, K., Hasselmann, S., and Janssen, P. A. E. M.: Dynamics and Modelling of Ocean Waves, Cambridge University Press, Cambridge, UK, 536 pp., 1994.
Lionello, P. and Sanna, A.: Mediterranean wave climate variability and its links with NAO and Indian Monsoon, Clim. Dynam., 25, 611–623, 2005.
Lionello P., Cogo, S., Galati, M. B., and Sanna, A.: The Mediterranean surface wave climate inferred from future scenario simulations, Global Planet. Change, 63, 152–162, 2008.
Lund, R. and Reeves, J.: Detection of Undocumented Changepoints: A Revision of the Two-Phase Regression Model, J. Climate, 15, 2547–2554, 2002.
Mathiesen, M.: Estimation of Wave Height Duration Statistic, Coast. Eng., 23, 167–181, 1994.
Mathiesen M., Goda, Y., Hawkes, P. J., Mansard, E., Martin, M. J., Peltier, E., Thompson, E. F., and Van Vledder, G.: Recommended Practice for Extreme Wave Analysis, J. Hydr. Res., 32(6), 803–814, 1994.

Muir, L. R. and El-Shaarawi, A. H.: On the Calculation of Extreme Wave Heights, A Review, Ocean Eng., 13(1), 93–118, 1986.
Nakicenovic, N., Alcamo, J., Davis, G., de Vries, H. J., Fenham, J., et al.: Special Report on Emissions Scenarios, a Special Report of Working Group III of the IPCC, Cambridge University Press, Cambridge, UK and New York, NY, USA, 599 pp., 2000.
Pirazzoli, P. A. and Tomasin, A.: Recent Near-Surface Wind Changes In The Central Mediterranean And Adriatic Areas, Int. J. Climatol., 23, 963–973, 2003.
Signell, R. P., Carniel, S., Cavaleri, L., Chiggiato, J., Doyle, J., Pullen, J., and Sclavo, M.: Assessment of wind quality for oceanographic modelling in semi-enclosed basins, J. Marine Syst., 53, 217–233, 2005.
Simiu, E. and Heckert, N. A.: Extreme wind distribution tails: A "peaks-over-threshold" approach, J. Struct. Eng., 122, 539–547, 1996.
Smith, R. L.: Extreme value theory based on the *r* largest annual events, J. Hydrol., 86, 27–43, 1987.
Smith, R. L.: Extreme Value Analysis of Environmental Time Series: An Application to Trend Detection in Ground-Level Ozone, Stat. Sci., 4(4), 367–377, 1989.
Tanurdjaja, A.: Extreme wind studies in Singapore. An area with mixed weather system, JWEIA, Netherlands, 90, 1611–1630, 2002.
Uppala, S. M., Kallberg, P. W., Simmons, A. J., Andrae, U., Bechtold, V. D., Fiorino, M., Gibson, J. K., Haseler, J., Hernandez, A., Kelly, G. A., Li, X., Onogi, K., Saarinen, S., Sokka, N., Allan, R. P., Andersson, E., Arpe, K., Balmaseda, M. A., Beljaars, A. C. M., Van De Berg, L., Bidlot, J., Bormann, N., Caires, S., Chevallier, F., Dethof, A., Dragosavac, M., Fisher, M., Fuentes, M., Hagemann, S., Holm, E., Hoskins, B. J., Isaksen, L., Janssen, P. A. E. M., Jenne, R., McNally, A. P., Mahfouf, J. F., Morcrette, J. J., Rayner, N. A., Saunders, R. W., Simon, P., Sterl, A., Trenberth, K. E., Untch, A., Vasiljevic, D., Viterbo, P., and Woollen, J.: The ERA-40 re-analysis, Q. J. Roy. Meteorol. Soc., 131, 2961–3012, 2005.
WAM-DI Group: The WAM model – a Third Generation Ocean Wave Prediction Model, J. Phys. Oceanogr., 18, 1775–1810, 1988.
Wang, X. L. L.: Accounting for Autocorrelation in Detecting Mean shifts in Climate Data Series Using the Penalized Maximal *t* or *F* test, J. Appl. Meteor. Climatol., 47, 2423–2444, 2008.
Weissman, I.: Estimation of parameters and large quantities based on the *k* largest observations, J. Am. Stat. Assoc., 73, 812–815, 1978.

Table 1. Slope and intercept values of linear wave timeseries correction.

Coordinates	Slope *a*	Intercept *c*	Coordinates	Slope *a*	Intercept *c*	Coordinates	Slope *a*	Intercept *c*
38.50° N,08.00° E	1.920	0.199	38.50° N,12.50° E	2.639	−0.217	40.50° N,14.50° E	1.859	0.091
40.00° N,08.00° E	1.567	0.131	44.50° N,12.50° E	1.132	0.575	42.50° N,14.50° E	2.002	0.487
41.00° N,08.00° E	1.515	0.525	44.00° N,13.00° E	2.329	−0.011	36.50° N,15.00° E	1.431	0.218
43.00° N,09.00° E	1.618	0.144	44.50° N,13.00° E	2.401	0.051	38.50° N,15.50° E	2.876	0.175
39.00° N,10.00° E	1.640	0.257	45.00° N,13.00° E	1.655	0.027	42.50° N,15.50° E	2.193	−0.029
41.50° N,10.00° E	1.552	0.040	45.50° N,13.00° E	1.066	−0.053	38.00° N,16.50° E	1.468	0.016
43.50° N,10.00° E	1.062	0.106	41.00° N,13.50° E	1.510	0.184	38.50° N,17.50° E	2.620	−0.002
42.50° N,10.50° E	1.302	0.082	44.50° N,13.50° E	2.006	0.083	41.00° N,17.50° E	1.287	0.353
41.50° N,12.00° E	1.489	0.092	44.50° N,14.00° E	2.389	0.043	39.50° N,18.50° E	2.658	0.337

OSD

6, 2005–2036, 2009

Table 2. Five tests of significance based on Student's t distributions with $N-2$ degrees of freedom (df) and mean μ_x. Symbols μ, μ_{32} and μ_{10} indicate the population mean and the μ-estimators of the 32- and 10-yr samples.

Temporal interval	y-sample	Hypothesis rejection	df=$N-2$	Null-Hypothesis	(α-level, t^*)	(p, t-test)
1958–1989	Counts H_s	yes	30	Sample $\in$ population with zero-slope	(5%, 2.042)	(0.350%, 3.170)
1990–1999	Counts H_s	yes	8	Sample $\in$ population with zero-slope	(5%, 2.306)	(4.501%, 2.374)
1990–1999	Counts H_s	yes	8	μ_{32} and μ_{10} are estimators of μ	(5%, 2.306)	(1.453%, 3.106)
1958–1989	Annual averaged H_s	yes	30	Sample $\in$ population with zero-slope	(5%, 2.042)	(2.000%, 2.456)
1990–1999	Annual averaged H_s	yes	8	Sample $\in$ population with zero-slope	(5%, 2.306)	(1.780%, 2.972)
1990–1999	Annual averaged H_s	yes	8	μ_{32} and μ_{10} are estimators of μ	(5%, 2.306)	(0.025%, 6.247)

OSD

6, 2005–2036, 2009

Table 3. Results of three tests of significance at the 5% α-level and based on Student's t distributions with $N-2$ degrees of freedom (df) for four different geographical sites. The null-hypothesis of zero-slope refers to the trends of the annual H_s durations over the 50th, 75th and 90th percentiles.

Location and coordinates	h-sample percentile	Hypothesis rejection	df=$N-2$	Null-Hypothesis	(α-level, t^*)	(p, t-test)
Northern Adriatic (45.00° N,13.00° E)	50	No	40	Sample $\in$ population with zero-slope	(5%, 2.021)	(14.184%, 1.501)
	75	No				(26.192%, 1.139)
	90	No				(8.801%, 1.751)
Gulf of Naples (41.00° N,13.50° E)	50	No	40	Sample $\in$ population with zero-slope	(5%, 2.021)	(27.211%, 1.115)
	75	No				(51.264%, 0.664)
	90	No				(7.486%, 1.832)
Middle Adriatic (42.50° N,15.50° E)	50	Yes	40	Sample $\in$ population with zero-slope	(5%, 2.021)	(0.330%, 3.130)
	75	No				(88.002%, 0.152)
	90	No				(19.725%, 1.312)
Ionian Sea (38.00° N,16.50° E)	50	No	40	Sample $\in$ population with zero-slope	(5%, 2.021)	(24.031%, 1.193)
	75	No				(94.270%, 0.071)
	90	No				(13.123%, 1.546)

OSD
6, 2005–2036, 2009

Table 4. Site coordinates, return values $H_s^{(100)}$ and duration τ_{100} at the return period T_n=100 yr computed by the POT and the *r*max methods.

Location and coordinates	$H_s^{(100)}$ -POT-	τ_{100}^{POT} [h]	$H_s^{(100)}$ -*r*max-	$\tau_{100}^{r\,max}$[hours]
(41.50° N,12.00° E)	5.68 m	8.87	5.81 m	9.53
(38.00° N,16.50° E)	6.62 m	9.22	6.88 m	10.74
(44.50° N,12.50° E)	5.08 m	8.39	5.09 m	9.17

OSD

6, 2005–2036, 2009

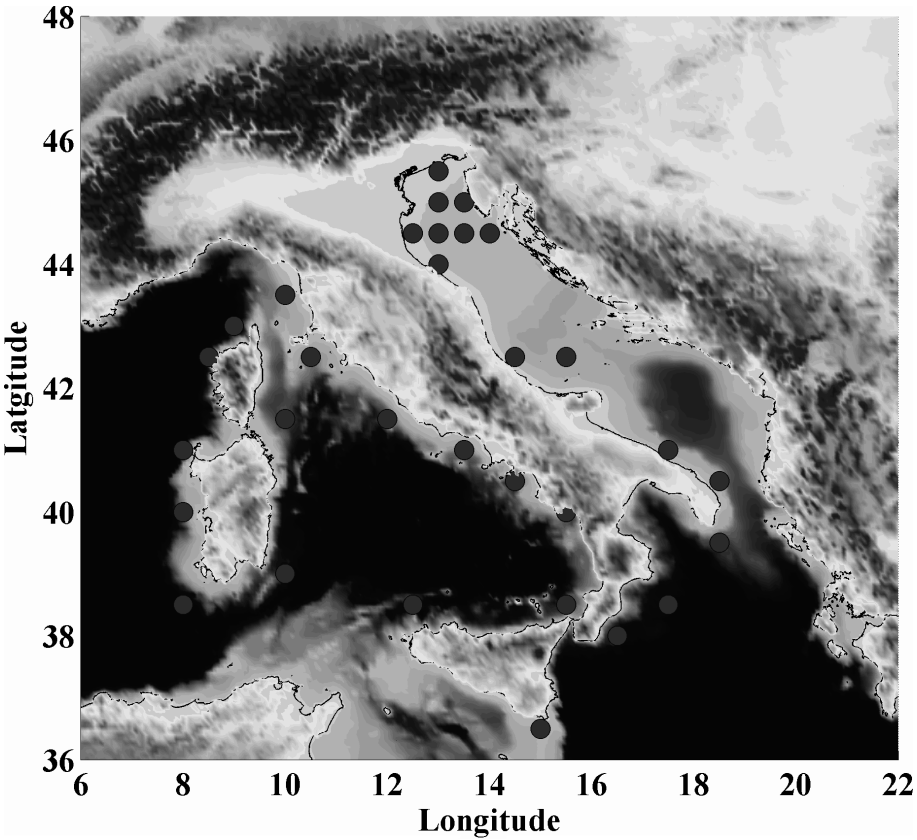

Fig. 1. The position of the 27 selected WAM-grid points (0.5° resolution) along the Italian coast. Points indicate the sites tested for the linear relation between calibrated ERA-40$_{UNILE}$ and ISMAR wave datasets.

OSD

6, 2005–2036, 2009

Statistical analysis and distribution of significant wave height

G. Martucci et al.

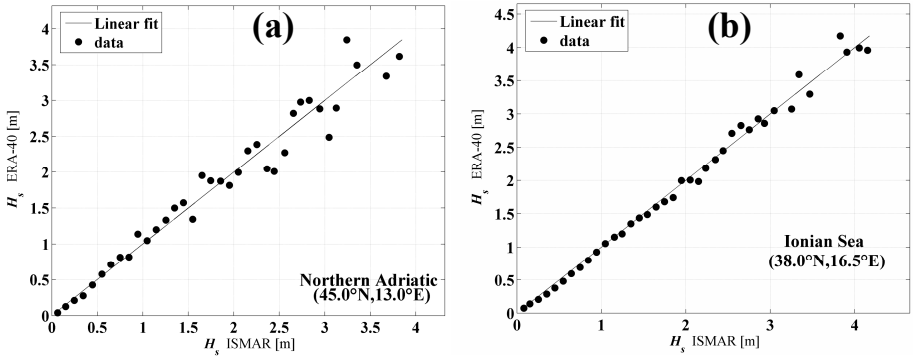

Fig. 2. Calibrated ERA-40$_{\text{UNILE}}$ significant wave height vs. ISMAR significant wave height. Data in the graphics have been averaged over a height-span of 0.1 m. The overlapped time interval between the ERA-40$_{\text{UNILE}}$ and the ISMAR timeseries goes from 1 July 1992 to 31 December 1999.

OSD

6, 2005–2036, 2009

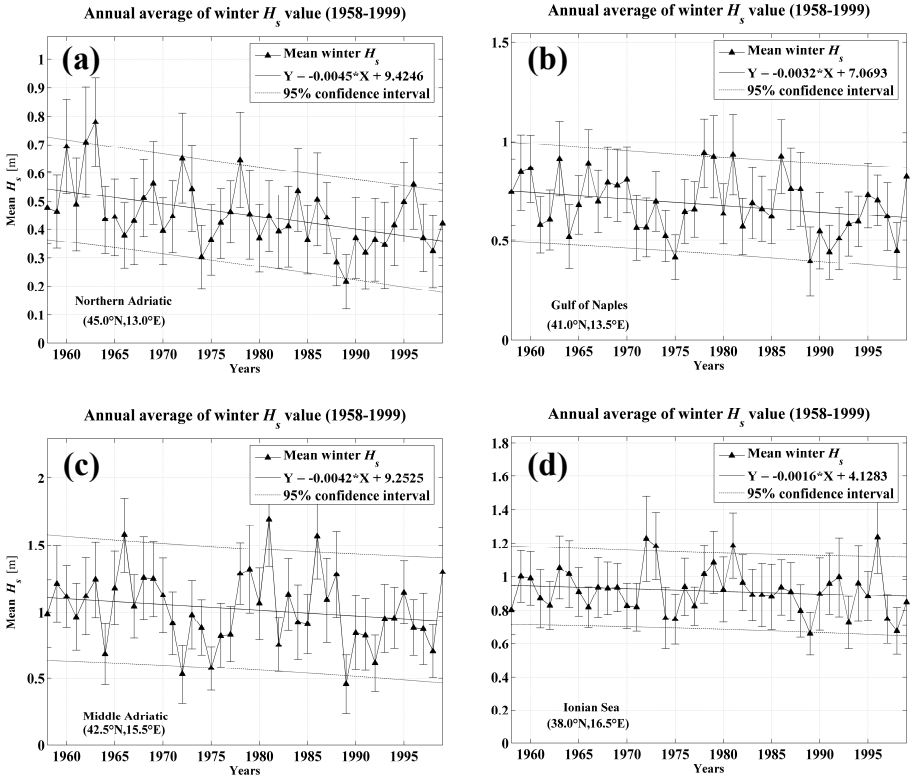

Fig. 3a. From **(a)** to **(d)**, at four different geographical sites, the winter-averaged H_s values through the 1958–1999. The strait solid line represents the linear regression of the timeseries with 95%-confidence intervals (dashed dotted-line). Error bars on *y*-values have amplitude equal to two times the H_s standard deviations. The four trends are statistically significant at the 5%-level of a Student's *t*.

OSD
6, 2005–2036, 2009

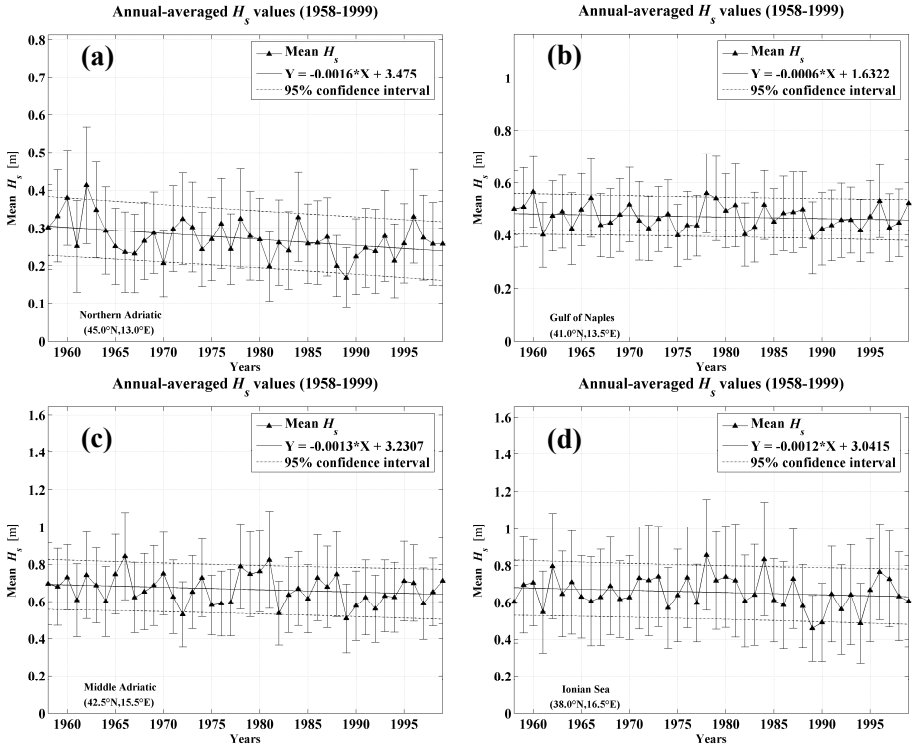

Fig. 3b. From **(a)** to **(d)**, at the same geographical sites as Fig. 3a, the annual-averaged H_s values through 1958–1999. The strait solid line represents the linear regression of the timeseries with 95%-confidence intervals (dashed dotted-line). Error bars on y-values have amplitude equal to two times the H_s standard deviations. The four trends are statistically significant at the 5%-level of a Student's t.

OSD
6, 2005–2036, 2009

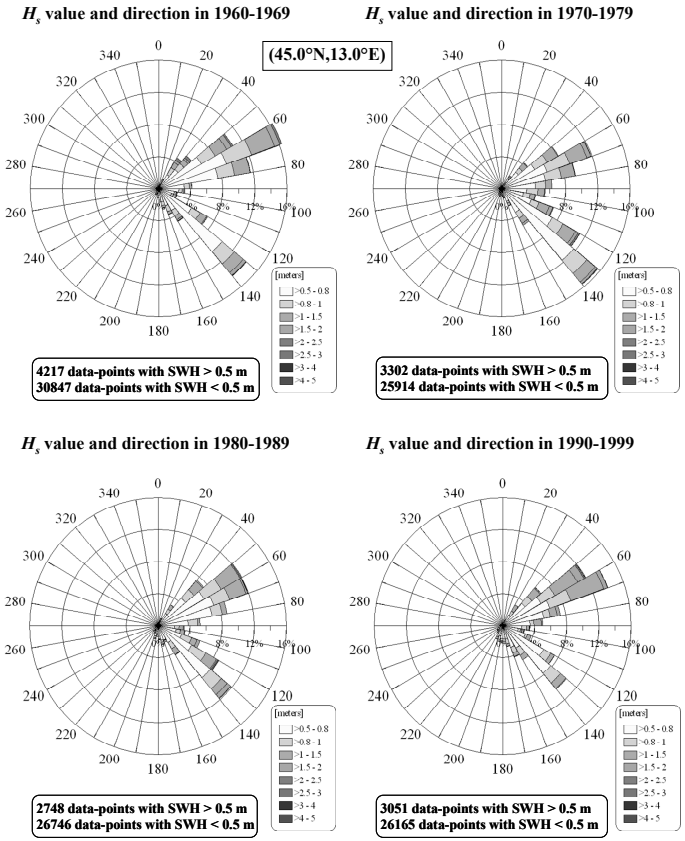

Fig. 4. Decennial rose diagrams from 1960 to 1999 of significant wave heights and relative frequencies of occurrence at (45.0° N, 13.0° E). The H_s values are filtered for heights <0.5 m.

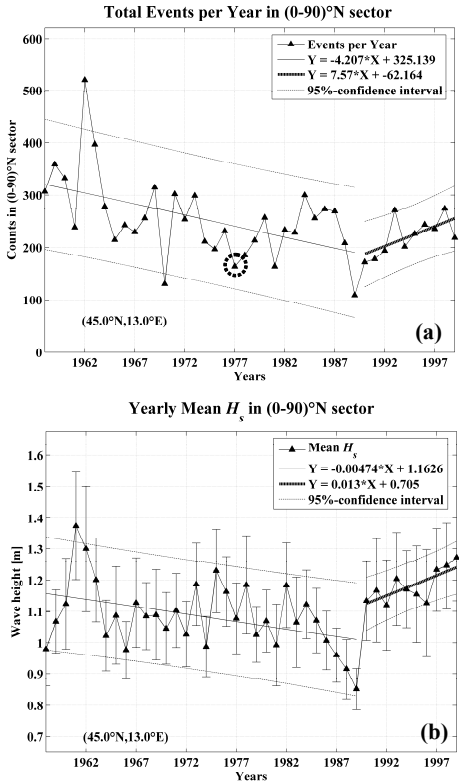

Fig. 5. Panel **(a)** and panel **(b)** show, for the period 1958–1999, respectively, the annual total number of sea-states and the mean annual H_s values in the sector of (0–90° N) incoming wave direction. Two linear fits for each panel display the trends over the year ranges 1958–1989 and 1990–1999. Dash-dotted lines around the regression lines indicates the 95%-confidence intervals. The circle in panel (a) shows the first turning-point in 1977. Error bars on panel (b) have amplitude equal to two times the annual H_s standard deviations.

OSD
6, 2005–2036, 2009

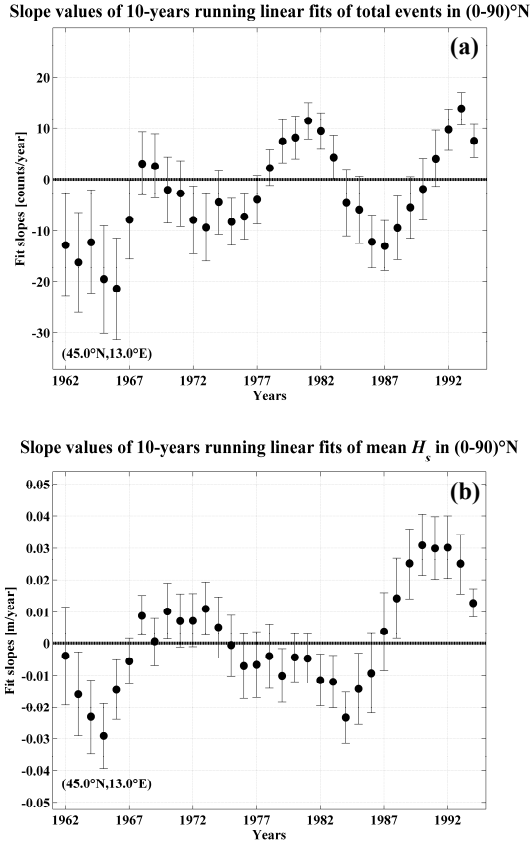

Fig. 6. Panel **(a)** and **(b)** show the slopes of the 10-yr running linear fits of, respectively, the total number of sea states and the mean annual H_s values as shown in Fig. 5a and b. The ith data point represents the slope of the linear regression through the years from $i-5$ to $i+5$. Error bars in both panels are equal to $\pm\sigma$.

OSD
6, 2005–2036, 2009

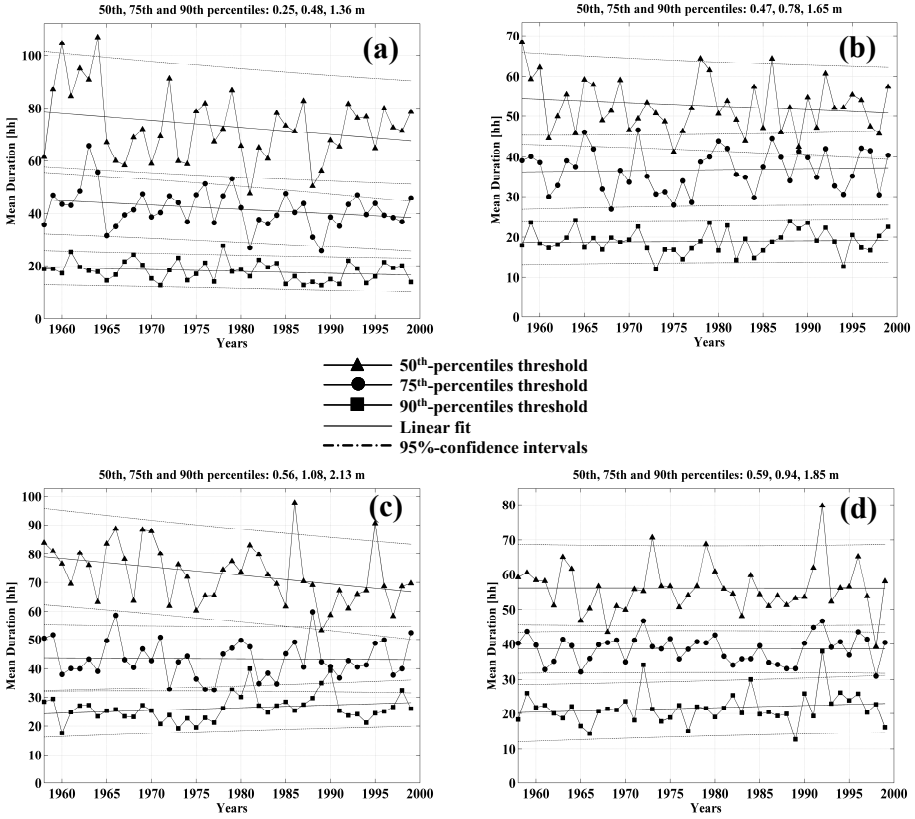

Fig. 7. From panel **(a)** to **(d)**, in the same order as for Fig. 3a, are shown the annual averaged H_s durations over three thresholds: the 50th, 75th and the 90th percentiles of the (ascending) ordered ERA-40$_{\text{UNILE}}$ dataset. A linear fit is also shown.

OSD
6, 2005–2036, 2009

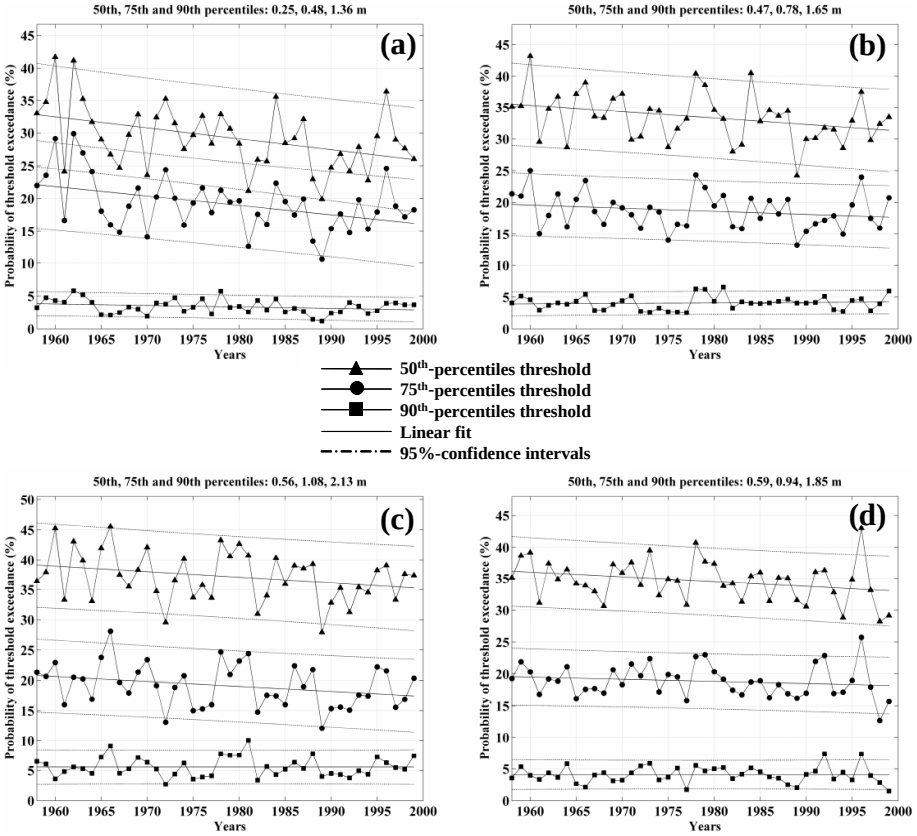

Fig. 8. From panel **(a)** to **(d)**, in the same order as for Fig. 3a, are shown the annual averaged H_s probabilities of exceeding three different thresholds set at the 50th, 75th and the 90th percentiles of the (ascending) ordered ERA-40$_{UNILE}$ dataset. Data are linearly fitted in order to highlight trends.

OSD
6, 2005–2036, 2009

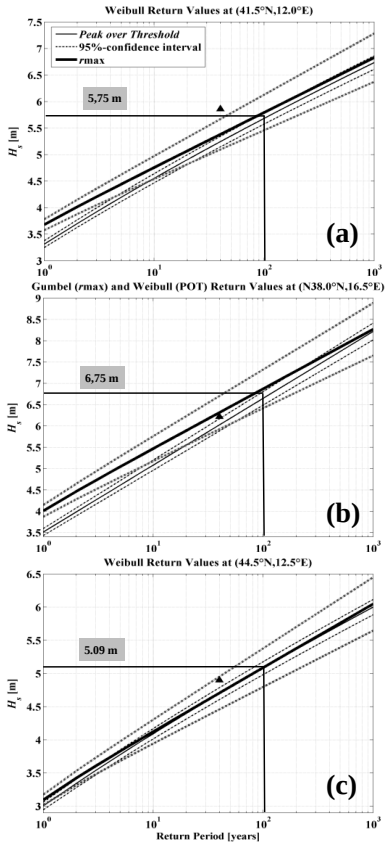

Fig. 9. From 1 to 1000 yr, the solid lines show the return values [m] obtained using the POT (thin) and the *r*-largest (thick) annual maxima methods. 95% confidence limits are also shown in thin/thick dashed lines. Black triangle have *y*-value equal to the *iid* maximum and *x*-value equal to T_n=40 yr. The two methods converge for return periods T_n>100 yr.

OSD
6, 2005–2036, 2009